FusedProp: Towards Efficient Training of Generative Adversarial Networks

Zachary Polizzi* South Park Commons

zplizzi@gmail.com

Chuan-Yung Tsai* South Park Commons

cytsai@gmail.com

Abstract

Generative adversarial networks (GANs) are capable of generating strikingly realistic samples but state-of-the-art GANs can be extremely computationally expensive to train. In this paper, we propose the fused propagation (FusedProp) algorithm which can be used to efficiently train the discriminator and the generator of common GANs simultaneously using only one forward and one backward propagation. We show that FusedProp achieves 1.49 times the training speed compared to the conventional training of GANs, although further studies are required to improve its stability. By reporting our preliminary results and open-sourcing our implementation, we hope to accelerate future research on the training of GANs.

1. Introduction

Generative adversarial networks (GANs) have been continually progressing the state-of-the-art in generative modeling of all kinds of data since its invention [4]. Among its many applications, image generation arguably has received the most attention due to its strikingly realistic results [7, 8, 9, 27, 2]. However, the training of these powerful GANs usually takes days to weeks even on high-end multi-GPU/-TPU machines, strongly limiting the number of experiments researchers can afford and negatively affecting the fairness and progress of the field.

To mitigate this challenge, existing work mainly relied on two types of acceleration. The first is to use lower numerical precision, *e.g.* half precision (fp16) instead of single precision (fp32) for training [7, 8, 9, 2]. The second is to adapt GAN's architecture using *e.g.* progressive growing [7], simplified normalization [9], shared embedding [21, 2], *etc.*

In this paper, we aim to accelerate the training procedure of GANs and propose the fused propagation (FusedProp) algorithm, a generalization of the gradient reversal algorithm [3] that can be used to train the discriminator and the generator of common GANs simultaneously using only one forward

and one backward propagation. Our algorithm offers $1.49\times$ the training speed compared to the conventional training of GANs and our code is publicly available. Although further studies are required to improve the stability of FusedProp, we hope our preliminary results and open-source implementation of FusedProp can accelerate future research on the training of GANs.

2. Background

The training of a GAN entails the minimax optimization of a two-player game between its discriminator D and its generator G defined as

$$\underset{G}{\operatorname{maxmin}} \ \mathcal{L}_{D}^{R}(D(x)) + \mathcal{L}_{D}^{F}(D(G(z))) \tag{1}$$

where G is trained (by maximizing \mathcal{L}_D^F) to map the latent variable z from a given (e.g. normal) distribution into G(z) that resembles the real data x such that D can not tell G(z) and x apart even if it is trained (by minimizing \mathcal{L}_D^R and \mathcal{L}_D^F) to do so. It is rather common to write the optimization of D and G separately as

$$\min_{D} \mathcal{L}_{D}^{R}(D(x)) + \mathcal{L}_{D}^{F}(D(G(z)))
\min_{G} \mathcal{L}_{G}(D(G(z)))$$
(2)

which allows for GAN losses with $\mathcal{L}_G \neq -\mathcal{L}_D^F$ and thus more desirable properties (e.g. stronger gradients using the nonsaturating loss [4], see Table 1 and its references for more details). For simplicity, we also write \mathcal{L}_D^F as \mathcal{L}_D in the rest of the paper.

$$\begin{split} \theta_D^{i+1} &= \theta_D^i - \alpha \frac{\partial \mathcal{L}_D^R(D(x;\theta_D^i)) + \mathcal{L}_D(D(G(z;\theta_G^i);\theta_D^i))}{\partial \theta_D^i} \\ \theta_G^{i+1} &= \begin{cases} \theta_G^i - \alpha \frac{\partial \mathcal{L}_G(D(G(z;\theta_G^i);\theta_D^i))}{\partial \theta_G^i} & \text{(SimGD)} \\ \theta_G^i - \alpha \frac{\partial \mathcal{L}_G(D(G(z;\theta_G^i);\theta_D^{i+1}))}{\partial \theta_G^i} & \text{(AltGD)} \end{cases} \end{split}$$

^{*}Equal contribution.

https://github.com/zplizzi/fusedprop

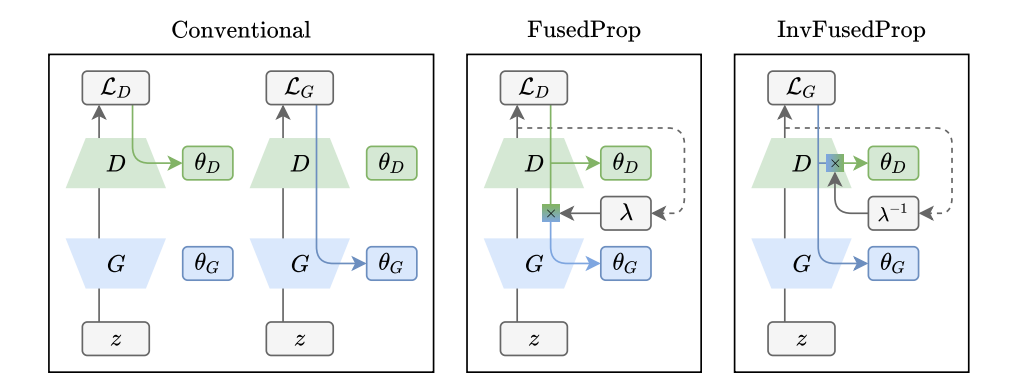


Figure 1. Conventional vs. fused propagation (FusedProp) and inverted fused propagation (InvFusedProp) training of GANs, where gray arrow indicates forward propagation, colored arrow indicates backward propagation and dashed arrow indicates conditional dependency. \mathcal{L}_D^R is omitted for simplicity.

	\mathcal{L}_D^R	$\mathcal{L}_D = \mathcal{L}_D^F$	\mathcal{L}_G	λ	λ^{-1}
Minimax [4]	softplus(-y)	softplus(y)	$-\operatorname{softplus}(y)$	-1	-1
Nonsaturating [4]	softplus(-y)	softplus(y)	softplus(-y)	$-e^{-y}$	$-e^y$
Wasserstein [1]	-y	y	-y	-1	-1
Least Squares [13]	$(y-1)^2$	y^2	$(y-1)^2$	$1 - y^{-1}$	$y \cdot (y-1)^{-1}$
Hinge [12, 24]	ReLU(-y+1)	ReLU(y+1)	-y	∄	-H(y+1)

Table 1. Common GAN losses and corresponding gradient scaling factors for FusedProp and InvFusedProp, where softplus $(x) = \ln(1 + e^x)$, ReLU $(x) = \max(x, 0)$ and H denotes the Heaviside step function.

Although the training of D and G is often described as simultaneous, it is rarely the case in practice. Specifically, instead of updating θ_D and θ_G simultaneously using SimGD [14] as defined in Eq. (3),² updating them alternatingly using AltGD [14] (often with multiple θ_D updates per θ_G update) is much more common, partly due to the stability and convergence concerns about SimGD [23, 15, 14]. However, researchers' view about SimGD is not unilaterally pessimistic since [19, 6] proved SimGD can lead to stable convergence of GANs as well. Encouraged by the positive results, we seek to accelerate the training of GANs based on the SimGD approach.

Of course, SimGD itself is not more computationally efficient than AltGD if one still needs to compute gradients for θ_D and θ_G using two backpropagations. Fortunately, it is known that if $\mathcal{L}_G = \bar{\lambda}\mathcal{L}_D$ for some constant $\bar{\lambda}$ (e.g. $\bar{\lambda} = -1$ as in the minimax loss), the gradient reversal algorithm [3] originally designed for the domain adaptation problem can be used to combine the two backpropagations by inserting a

simple function GR defined as

$$GR_{\bar{\lambda}}(x) = x$$

$$\frac{\partial GR_{\bar{\lambda}}(x)}{\partial x} = \bar{\lambda}I$$
(4)

between D and G.⁴ Inspired by the gradient reversal algorithm, we aim to bring its level of efficiency to the training of GANs while supporting a broader set of GAN losses.

3. Algorithm

Although [3] also mentioned the possibility of generalizing the gradient reversal algorithm to arbitrary GAN losses, it is unclear if such generalization can be implemented as efficiently. To this end, we formally derive the fused propagation (FusedProp) algorithm, a generalization of the gradient reversal algorithm for common GAN losses, and outline its implementation in the rest of the section.

The first form of FusedProp closely follows the gradient reversal algorithm, except with a data-dependent gradient

 $^{^2 \}text{Where } D(x) \text{ and } G(z) \text{ are written more precisely as } D(x;\theta_D) \text{ and } G(z;\theta_G) \text{ and stochastic gradient descent (SGD, instead of Adam) with learning rate } \alpha \text{ is used for simplicity.}$

³Which is equivalent to AltGD (*i.e.* conventional) in Fig. 1 except that the update for θ_D is delayed (till the update for θ_G) and z is reused (instead of redrawn for the second forward propagation).

⁴However, as also noted in [25], using the gradient reversal algorithm with a common setting of $\bar{\lambda}=-1$ (*i.e.* the minimax loss) to train GANs is not ideal [4], which may explain the lack of such attempts in the literature.

```
class FusedProp(torch.autograd.Function):
  @staticmethod
  def forward(ctx, Gz):
    return Gz
  @staticmethod
  def backward(ctx, gGz):
    # F1. get _lambda (calculated globally)
    global _lambda
    # F2. scale gGz (gradient of Gz) as Eq. (4)
    return gGz * _lambda.view(-1, 1, 1, 1)
# P1. forward D & G once with FusedProp
x_Gz = torch.cat(x, FusedProp.apply(G(z)))
yr, yf = D(x_Gz).chunk(2)
# P2. calculate loss (nonsaturating) and _lambda
loss_ns = F.softplus(-yr) + F.softplus(yf)
_{lambda} = -((-yf).exp())
# P3. backward D & G once to get all gradients
loss_ns.mean().backward()
# P4. update D & G simultaneously
optimizer_D_G.step()
```

Figure 2. PyTorch example of FusedProp training, where P1-P4 describe the procedure of one training iteration and F1-F2 describe the FusedProp steps.

scaling factor λ for certain GAN losses. As shown below

$$\frac{\partial \mathcal{L}_{G}}{\partial \theta_{G}} = \frac{\partial \mathcal{L}_{G}}{\partial \mathcal{L}_{D}} \frac{\partial \mathcal{L}_{D}}{\partial G(z)} \frac{\partial G(z)}{\partial \theta_{G}} = \frac{\partial \mathcal{L}_{D}}{\partial G(z)} \underbrace{\frac{\partial \mathcal{L}_{G}}{\partial \mathcal{L}_{D}}}_{\lambda} \frac{\partial G(z)}{\partial \theta_{G}}$$
(5)

and in Fig. 1, instead of computing $\frac{\partial \mathcal{L}_G}{\partial \theta_G}$ with a second set of forward and backward propagations, one can⁵ scale $\frac{\partial \mathcal{L}_D}{\partial G(z)}$ (a byproduct of computing $\frac{\partial \mathcal{L}_D}{\partial \theta_D}$ during \mathcal{L}_D minimization) by λ to extend the first backward propagation to obtain $\frac{\partial \mathcal{L}_G}{\partial \theta_G}$, essentially fusing two sets of forward and backward propagations into one. A PyTorch example of FusedProp training is provided in Fig. 2. For common GAN losses where \mathcal{L}_D and \mathcal{L}_G are both univariate scalar functions (i.e. $\mathbb{R} \to \mathbb{R}$), λ can be easily derived because $\frac{\partial \mathcal{L}_G}{\partial \mathcal{L}_D} = \frac{\mathcal{L}_G'}{\mathcal{L}_D'}$. Table 1 summarizes λ for 5 such GAN losses, where λ is simply -1for the minimax and the Wasserstein loss as in the gradient reversal algorithm, and depends on y (the output of D) for the nonsaturating and the least squares loss. The hinge loss however is not supported by this form of FusedProp, as the zero derivative part of ReLU leaves λ undefined (division by zero).

To circumvent the problem of the hinge loss, we propose the second form of FusedProp, the inverted FusedProp (InvFusedProp). As shown below

$$\frac{\partial \mathcal{L}_D}{\partial \theta_D} = \frac{\partial \mathcal{L}_D}{\partial \mathcal{L}_G} \frac{\partial \mathcal{L}_G}{\partial \theta_D} = \frac{\partial \mathcal{L}_G}{\partial \theta_D} \underbrace{\frac{\partial \mathcal{L}_D}{\partial \mathcal{L}_G}}_{\text{j-1}}$$
(6)

```
class InvFusedPropLinear(torch.autograd.Function):
  @staticmethod
  def forward(ctx, x, W, b):
    ctx.save_for_backward(x, W)
    y = x.matmul(W.t()) + b
    return y
  @staticmethod
  def backward(ctx, gy):
    x, W = ctx.saved_tensors
    # I1. get _lambda_inv (calculated globally)
    global _lambda_inv
    # I2. pre-scale gy (gradient of y)
    scaled_gy = gy * _lambda_inv.view(-1, 1)
    # I3. Compute gradients for
          activation (x) with gy
          parameters (W & b) with scaled gy
    gx = gy.matmul(W)
    gW = scaled_gy.t().matmul(x)
    gb = scaled_gy.sum(0)
    return gx, gW, gb
```

Figure 3. PyTorch example of InvFusedProp-based linear (*i.e.* fully connected) layer, where I1-I3 describe the InvFusedProp steps. See our code for examples of other types of layers.

and in Fig. 1, one can also obtain $\frac{\partial \mathcal{L}_D}{\partial \theta_D}$ during \mathcal{L}_G minimization. tion by scaling the "incorrect" gradient $\frac{\partial \mathcal{L}_G}{\partial \theta_D}$ by λ^{-1} . Worth to note, unlike FusedProp which can be trivially done in most deep learning frameworks, InvFusedProp requires additional effort to implement correctly and efficiently. This is due to the fact that λ^{-1} takes different values for different data in a batch, but in most frameworks gradients for parameters (here $\frac{\partial \mathcal{L}_D}{\partial \theta_D}$) are only available as already reduced across all data in a batch for performance reasons. Instead, one should pre-scale the gradient by λ^{-1} before computing gradients for parameters within each layer of D. A PyTorch example of InvFusedProp-based layer is provided in Fig. 3. InvFused-Prop is slightly slower than FusedProp as additional scaling operations are needed in all layers of D. For GAN losses with valid but different λ and λ^{-1} (e.g. the nonsaturating and the least squares loss), it is also possible to adaptively switch between the two forms if the numerical accuracy of one is better than the other.⁷

Both forms of the FusedProp algorithm are exact and efficient implementations of the SimGD-based training of GANs, which bring the conventional time complexity of $\mathcal{O}(6T_D+3T_G)$ down to $\mathcal{O}(4T_D+2T_G)$, where T_D and T_G stand for the time complexities of the forward and backward propagations of D and G respectively. As D and G

 $^{^5\}mbox{Due}$ to the commutative property of the scalar and (Jacobian) matrix product.

⁶E.g. for convolutional layers, we need to use MKL-DNN or CuDNN subroutines for InvFusedProp to ensure performance.

 $^{^{7}}E.g.$ when using fp16 for training. We do not observe such need using fp32 in our experiments.

⁸This assumes \mathcal{L}_D^R , \mathcal{L}_D and \mathcal{L}_G are all using the same batch size, and the gradients for parameters and activation within each layer are computed in parallel. If computed in serial, time complexities are $\mathcal{O}(8T_D+4T_G)$ vs. $\mathcal{O}(6T_D+3T_G)$.



Figure 4. Unconditional CIFAR10 image generation using Fused-Prop-trained GANs, where subfigures (numbered from top to bottom) come from experiments specified in Table 2.

are commonly of similar complexity (i.e. $T_D \approx T_G$), we can expect approximately $1.5\times$ theoretical speedup by using FusedProp training. SimGD-based training of GANs however is not guaranteed to match the results of the conventional AltGD-based training, thus needs to be experimentally validated too.

4. Experiments

In this paper, we closely follow the setup of [17], *i.e.* unconditional CIFAR10 image generation using CNN or ResNet-based GANs with nonsaturating or hinge loss to validate the FusedProp algorithm. We perform 5 runs for all configurations and summarize their Inception Scores (IS), Frchet Inception Distances (FID) and speed⁹ in Table 2. Samples from the FusedProp-trained GANs are provided in Fig. 4.

For CNN-based experiments, we choose the learning rate pair that performed the best in [17, 11] and find no significant difference in terms of IS and FID between conventional and FusedProp training. For ResNet-based experiments, we first adopt the TTUR [6] learning rate pair 10 used by [27] but find that FusedProp training performs significantly worse than conventional training in this setting. With some manual tuning, we are able to stabilize FusedProp training and eliminate the difference in terms of IS and FID by halving the learning rate of G, which unfortunately also increases conventional training's FID, making this setting similar to [11] but likely worse than [17]. On the other hand, we do observe sizable speedups using FusedProp training in all settings, ranging from $1.45 \times$ to $1.55 \times$ (overall $1.49 \times$) which

match the theoretical analysis.

Other factors that may cause a difference between conventional and FusedProp training are as follows. First, conventional training implicitly uses twice the amount of power iterations in the spectral normalization compared to FusedProp. Second, conventional training uses twice the amount of generated images in each iteration by redrawing z compared to FusedProp.³ However, we do not observe meaningful changes in the IS and FID when we correct conventional or FusedProp training to match each other in these two regards, implying that the fundamental difference between AltGD and SimGD-based training is the root cause here. ¹¹

5. Discussion

Although our preliminary results indicate that FusedProp is not exactly a drop-in replacement for conventional training of GANs as it may require additional hyperparameter tuning due to SimGD's different nature, we hope that as more researchers start to realize and utilize its computational efficiency, more research will follow to fundamentally solve the issues of SimGD-based training. At the same time, it will be crucial in our future work to study if existing techniques [14, 26] can be efficiently combined with FusedProp to improve its stability for larger-scale problems.

The FusedProp algorithm also has known limitations, which we list as follows.

- 1. FusedProp does not provide much speedup if multiple θ_D updates are required per θ_G update [1, 5]. We find TTUR an effective replacement in our experiments and recommend using it instead, as also advocated by [27].
- 2. Gradient penalties on D that involve G(z), including [5, 10] and the R2 penalty [14], are not compatible with FusedProp as their second-order gradients can incorrectly affect G. The increasingly popular R1 penalty [14, 8, 9] however is compatible.
- 3. Most conditional GANs [16, 22, 18] are compatible with FusedProp. However, ones that explicitly use a classification loss in addition to the GAN loss [20] are not compatible as gradients from those two losses become inseparable to be correctly scaled.

References

- [1] Martin Arjovsky, Soumith Chintala, and Léon Bottou. Wasserstein generative adversarial networks. In *ICML*, 2017. 2, 4
- [2] Andrew Brock, Jeff Donahue, and Karen Simonyan. Large scale GAN training for high fidelity natural image synthesis. In *ICLR*, 2019. 1
- [3] Yaroslav Ganin and Victor Lempitsky. Unsupervised domain adaptation by backpropagation. In *ICML*, 2015. 1, 2

 $^{^9}$ Measured in iterations per second at batch size of 64 for \mathcal{L}^R_D , \mathcal{L}_D and \mathcal{L}_G using one V100 GPU.

 $^{^{10}}$ Instead of multiple θ_D updates per θ_D update as suggested by [11] which we do not currently support.

¹¹We have also tested SimGD without the FusedProp acceleration and obtained the same results as FusedProp, suggesting this is not due to any flaw in FusedProp.

Architecture	(D,G) LRs	Loss	Training	IS [23]	FID [6]	Speed ⁹	Speedup	Samples
CNN	$(2.0,2.0) \times 10^{-4}$	NS	С	7.21 ± 0.06	27.23 ± 0.96	26.9		
			F	7.17 ± 0.05	27.91 ± 0.60	41.7	$1.55 \times$	Fig. 4.1
		HG	C	7.32 ± 0.12	25.42 ± 1.53	27.0		
			I	7.32 ± 0.07	24.59 ± 1.13	40.4	$1.50 \times$	Fig. 4 .2
ResNet	$(4.0,1.0) \times 10^{-4}$	NS	С	7.66 ± 0.20	22.65 ± 1.50	14.9		
			F	3.08 ± 0.37	118.2 ± 14.7	21.9	$1.47 \times$	
		HG	C	7.68 ± 0.15	19.93 ± 1.66	14.6		
			I	4.11 ± 0.39	94.00 ± 6.32	21.1	$1.45 \times$	
ResNet	$(4.0,0.5) \times 10^{-4}$	NS	C	7.59 ± 0.14	27.56 ± 1.17			
			F	7.55 ± 0.22	26.97 ± 1.67			Fig. 4.3
		HG	C	7.76 ± 0.15	23.41 ± 1.15			
		пО	I	7.66 ± 0.11	23.49 ± 0.79			Fig. 4.4

Table 2. Unconditional CIFAR10 image generation results using conventional (C), FusedProp (F) or InvFusedProp (I) training, nonsaturating (NS) or hinge (HG) loss, and Adam optimizer at specified learning rates (LRs).

- [4] Ian Goodfellow, Jean Pouget-Abadie, Mehdi Mirza, Bing Xu, David Warde-Farley, Sherjil Ozair, Aaron Courville, and Yoshua Bengio. Generative adversarial nets. In *NeurIPS*, 2014. 1, 2
- [5] Ishaan Gulrajani, Faruk Ahmed, Martin Arjovsky, Vincent Dumoulin, and Aaron C Courville. Improved training of Wasserstein GANs. In *NeurIPS*, 2017. 4
- [6] Martin Heusel, Hubert Ramsauer, Thomas Unterthiner, Bernhard Nessler, and Sepp Hochreiter. GANs trained by a two time-scale update rule converge to a local Nash equilibrium. In *NeurIPS*, 2017. 2, 4, 5
- [7] Tero Karras, Timo Aila, Samuli Laine, and Jaakko Lehtinen. Progressive growing of GANs for improved quality, stability, and variation. In *ICLR*, 2018. 1
- [8] Tero Karras, Samuli Laine, and Timo Aila. A style-based generator architecture for generative adversarial networks. In *CVPR*, 2019. 1, 4
- [9] Tero Karras, Samuli Laine, Miika Aittala, Janne Hellsten, Jaakko Lehtinen, and Timo Aila. Analyzing and improving the image quality of StyleGAN. arXiv, 2019. 1, 4
- [10] Naveen Kodali, Jacob Abernethy, James Hays, and Zsolt Kira. On convergence and stability of GANs. *arXiv*, 2017. 4
- [11] Karol Kurach, Mario Lucic, Xiaohua Zhai, Marcin Michalski, and Sylvain Gelly. A large-scale study on regularization and normalization in GANs. In *ICML*, 2019. 4
- [12] Jae Hyun Lim and Jong Chul Ye. Geometric GAN. arXiv, 2017. 2
- [13] Xudong Mao, Qing Li, Haoran Xie, Raymond YK Lau, Zhen Wang, and Stephen Paul Smolley. Least squares generative adversarial networks. In *ICCV*, 2017. 2
- [14] Lars Mescheder, Andreas Geiger, and Sebastian Nowozin. Which training methods for GANs do actually converge? In *ICML*, 2018. 2, 4
- [15] Lars Mescheder, Sebastian Nowozin, and Andreas Geiger. The numerics of GANs. In *NeurIPS*, 2017.
- [16] Mehdi Mirza and Simon Osindero. Conditional generative adversarial nets. arXiv, 2014. 4

- [17] Takeru Miyato, Toshiki Kataoka, Masanori Koyama, and Yuichi Yoshida. Spectral normalization for generative adversarial networks. In *ICLR*, 2018. 4
- [18] Takeru Miyato and Masanori Koyama. cGANs with projection discriminator. In ICLR, 2018. 4
- [19] Vaishnavh Nagarajan and J Zico Kolter. Gradient descent GAN optimization is locally stable. In *NeurIPS*, 2017.
- [20] Augustus Odena, Christopher Olah, and Jonathon Shlens. Conditional image synthesis with auxiliary classifier GANs. In *ICML*, 2017. 4
- [21] Ethan Perez, Florian Strub, Harm De Vries, Vincent Dumoulin, and Aaron Courville. Film: Visual reasoning with a general conditioning layer. In *AAAI*, 2018. 1
- [22] Scott Reed, Zeynep Akata, Xinchen Yan, Lajanugen Logeswaran, Bernt Schiele, and Honglak Lee. Generative adversarial text to image synthesis. In *ICML*, 2016. 4
- [23] Tim Salimans, Ian Goodfellow, Wojciech Zaremba, Vicki Cheung, Alec Radford, and Xi Chen. Improved techniques for training GANs. In *NeurIPS*, 2016. 2, 5
- [24] Dustin Tran, Rajesh Ranganath, and David Blei. Hierarchical implicit models and likelihood-free variational inference. In *NeurIPS*, 2017. 2
- [25] Eric Tzeng, Judy Hoffman, Kate Saenko, and Trevor Darrell. Adversarial discriminative domain adaptation. In CVPR, 2017.
 2
- [26] Maciej Wiatrak and Stefano V Albrecht. Stabilizing generative adversarial network training: A survey. arXiv, 2019.
- [27] Han Zhang, Ian Goodfellow, Dimitris Metaxas, and Augustus Odena. Self-attention generative adversarial networks. In ICML, 2019. 1, 4